New Indides $Sc_6Co_{2.18}In_{0.82}$, $Sc_{10}Ni_9In_{19.44}$ and $ScCu_4In$ – Synthesis, Structure, and Crystal Chemistry

Roman I. Zaremba[a], Yaroslav M. Kalychak[b], Ute Ch. Rodewald[a], Rainer Pöttgen[a], and Vasyl' I. Zaremba[b]

[a] Institut für Anorganische und Analytische Chemie, Westfälische Wilhelms-Universität Münster, Corrensstraße 30, 48149 Münster, Germany
[b] Inorganic Chemistry Department, Ivan Franko National University of Lviv, Kyryla and Mephodiya Street 6, 79005 Lviv, Ukraine

Reprint requests to R. Pöttgen. E-mail: pottgen@uni-muenster.de

Z. Naturforsch. **61b,** 942 – 948 (2006); received May 9, 2006

New indides $Sc_6Co_{2.18}In_{0.82}$, $Sc_{10}Ni_9In_{19.44}$ and $ScCu_4In$ have been synthesized from the elements by arc-melting. Single crystals were grown by special annealing modes. The thee indides were investigated *via* X-ray powder and single crystal diffraction: Ho_6Co_2Ga type, *Immm*, $a = 886.7(3)$, $b = 878.0(2)$, $c = 932.1(3)$ pm, $wR2 = 0.0517$, 711 F^2 values, 35 variables for $Sc_6Co_{2.18}In_{0.82}$, $Ho_{10}Ni_9In_{20}$ type, $P4/nmm$, $a = 1287.5(2)$, $c = 884.7(1)$ pm, $wR2 = 0.0642$, 1221 F^2 values, 63 variables for $Sc_{10}Ni_9In_{19.44}$, and $MgCu_4Sn$ type, $F\bar{4}3m$, $a = 704.03(7)$ pm, $wR2 = 0.0267$, 101 F^2 values, and 7 variables for $ScCu_4In$. The scandium rich indide $Sc_6Co_{2.18}In_{0.82}$ contains two Co_2 dumb-bells at Co–Co distances of 221 and 230 pm. Each cobalt atom within these dumb-bells has a tricapped trigonal prismatic coordination. The In1 site has a distorted cube-like coordination by scandium and shows a mixed occupancy (36%) with cobalt. The In2 atoms have distorted icosahedral scandium coordination. As a consequence of the small size of the scandium atoms, the In4 site in $Sc_{10}Ni_9In_{19.44}$ shows defects and was furthermore refined with a split model leading to a new distorted variant within the family of $Ho_{10}Ni_9In_{20}$ compounds. $ScCu_4In$ is an ordered version of the cubic Laves phase with scandium and indium atoms in the CN16 voids of the copper substructure. The Cu–Cu distances within the three-dimensional network of corner-sharing tetrahedra are 248.6 and 249.2 pm. The crystal chemical peculiarities of these three indide structures are briefly discussed.

Key words: Scandium, Intermetallics, Crystal Chemistry, Chemical Bonding

Introduction

Although scandium has a significantly smaller metallic radius (161 pm) than the smallest rare earth element lutetium (173 pm) [1], scandium sometimes forms intermetallic compounds that are isotypic with those of the rare earth elements [2]. So far, the indides $ScNi_4In$ ($MgCu_4Sn$ type) [3], ScT_2In (T = Ni, Cu, Pd, Ag, Pt, Au) ($MnCu_2Al$ type) [4 – 6], Sc_2T_2In (T = Ni, Cu, Pd, Au) (Mo_2FeB_2 or U_2Pt_2Sn type) [7, 8], ScPtIn with ZrNiAl structure [9], $Sc_5Ni_2In_4$ and $Sc_5Rh_2In_4$ with $Lu_5Ni_2In_4$ type [10], the $Lu_3Co_{1.87}In_4$ related indides $Sc_3Ni_{2-x+y}In_{4-y}$ ($x = 0.10$, $y = 0.24$ and $x = 0.30$, $y = 0.40$), $ScPd_{0.981}In$, and $Sc_3Rh_{1.593}In_4$ [11], and a solid solution $Sc_{1-x}PdIn_x$ [12] with CsCl structure have been reported.

Of all rare earth–transition metal–indium systems, however, those with scandium have only been scarcely investigated. We have now started a more systematic study of the scandium–transition metal–indium systems with respect to the crystal chemical peculiarities. The synthesis and structures of new indides $Sc_6Co_{2.18}In_{0.82}$, $Sc_{10}Ni_9In_{19.44}$ and $ScCu_4In$ are reported herein.

Experimental Section

Synthesis

Starting materials for the preparation of the Sc_6Co_2In, $Sc_{10}Ni_9In_{20}$ and $ScCu_4In$ samples were scandium ingots (Kelpin), cobalt powder (Sigma-Aldrich, 100 mesh), nickel wire (∅0.38 mm, Johnson Matthey), copper wire (Johnson Matthey, ∅1 mm), and indium tear drops (Johnson-Matthey), all with stated purities better than 99.9%. Small scandium pieces were arc-melted [13] in a first step under an argon pressure of *ca.* 600 mbar. This pre-melting procedure avoids shattering during the subsequent reactions with the other elements. The argon was purified over molecular sieves, silica gel and titanium sponge (900 K).

Table 1. Crystal data and structure refinement for $ScCu_4In$, $Sc_6Co_{2.18(1)}In_{0.82(1)}$ and $Sc_{10}Ni_9In_{19.44(1)}$.

Empirical formula	$ScCu_4In$	$Sc_6Co_{2.18(1)}In_{0.82(1)}$	$Sc_{10}Ni_9In_{19.44(1)}$
Structure type	$MgCu_4Sn$	Ho_6Co_2Ga	$Ho_{10}Ni_9In_{20}$
Z	4	4	2
Molar mass [g/mol]	413.94	492.52	3210.09
Space group	$F\bar{4}3m$	$Immm$	$P/4nmm$
Unit cell dimensions [pm]	$a = 704.03(7)$	$a = 886.7(3)$	$a = 1287.5(2)$
(Guinier powder data)		$b = 878.0(2)$	
		$c = 932.1(3)$	$c = 884.7(1)$
[nm^3]	$V = 0.3490$	$V = 0.7257$	$V = 1.4665$
Calculated density [g/cm^3]	7.88	4.51	7.27
Crystal size [μm^3]	$20 \times 30 \times 130$	$40 \times 45 \times 120$	$20 \times 20 \times 110$
Transm. ratio (max/min)	2.14	1.23	1.97
Absorption coefficient [mm^{-1}]	32.0	12.5	22.7
F(000)	744	900	2829
θ Range [°]	5 to 35	3 to 32	2 to 30
Range in *hkl*	± 11, ± 11, ± 11	± 13, ± 12, ± 13	$+18$, ± 18, ± 12
Total no. reflections	1470	4561	4708
Independent reflections	101	711	1221
	($R_{\rm int} = 0.0763$)	($R_{\rm int} = 0.1076$)	($R_{\rm int} = 0.0637$)
Reflections with $I > 2\sigma(I)$	101	535	921
	($R_\sigma = 0.0212$)	($R_\sigma = 0.0558$)	($R_\sigma = 0.0484$)
Data/parameters	101 / 7	711 / 35	1221 / 63
Goodness-of-fit on F^2	1.238	1.016	1.028
Final R indices [$I > 2\sigma(I)$]	$R1 = 0.0105$	$R1 = 0.0284$	$R1 = 0.0307$
	$wR2 = 0.0267$	$wR2 = 0.0468$	$wR2 = 0.0580$
R Indices (all data)	$R1 = 0.0105$	$R1 = 0.0514$	$R1 = 0.0513$
	$wR2 = 0.0267$	$wR2 = 0.0517$	$wR2 = 0.0642$
Extinction coefficient	0.032(1)	0.0011(1)	0.00119(5)
Flack parameter	0.00(2)	–	–
Largest diff. peak and hole [e/Å^3]	0.68 / −0.72	2.09 / −1.09	2.37 / −2.15

The small scandium buttons were then mixed with the transition metal and pieces of the indium tear drops in the ideal 6 : 2 : 1, 10 : 9 : 20, and 1 : 4 : 1 atomic ratios and the mixtures were subsequently melted in the same arc-melting furnace. The product pellets were turned over and remelted three times in order to ensure homogeneity. The weight losses after the different melting steps were always smaller than 0.5 weight-%. The samples are stable in air for months. No deterioration was observed. Powders of these indides are dark grey and the single crystals exhibit metallic lustre.

Single crystals of Sc_6Co_2In and $Sc_{10}Ni_9In_{20}$ were grown using special heat treatment. First, the alloys were powdered and cold-pressed into pellets. Next, the samples were put in small tantalum containers that were sealed in evacuated silica tubes as an oxidation protection. The ampoules were first heated to 1290 K for the Co and to 1250 K for the Ni compound within 8 h and held at that temperature for 6 h. Subsequently, the temperature was lowered at rate 4 K/h to 970 K for the Co compound (to 870 K for the Ni compound), then at a rate of 10 K/h to 600 K for both compounds, and finally cooled to room temperature within 10 h. As a result, in both cases, single crystals of irregular shape were obtained. After cooling, the samples could easily be separated from tantalum containers. No reaction of the samples with tantalum could be detected. $ScCu_4In$ crystals were obtained from the arc-melted button.

X-ray film data and structure refinements

The samples were characterized through Guinier powder patterns using Cu-$K_{\alpha 1}$ radiation and α-quartz ($a = 491.30$, $c = 540.46$ pm) as an internal standard. The Guinier camera was equipped with an imaging plate system (Fujifilm BAS–1800). The lattice parameters (Table 1) were obtained from least-squares fits of the X-ray powder data. Proper indexing was ensured through comparison with calculated patterns [14] using the atomic positions obtained from the structure refinements. The lattice parameters derived for the powders and the single crystals agreed well (Table 1).

Single crystals of the three indides were selected from the samples *via* mechanical fragmentation and examined by Laue photographs on a Buerger precession camera (equipped with an imaging plate system Fujifilm BAS–1800) in order to establish suitability for intensity data collection. Intensity data were collected at r. t. by use of a four-circle diffractometer (CAD4) with graphite monochromatized Mo-K_α radiation (71.073 pm) and a scintillation counter with pulse height discrimination. The scans were performed in the $\omega/2\theta$ mode. Empirical absorption corrections were applied on the basis of Ψ-scan data, followed by spherical absorption corrections. All relevant crystallographic data for the data collections and evaluations are listed in Table 1.

Table 2. Atomic coordinates and equivalent isotropic displacement parameters (pm^2) of $ScCu_4In$, $Sc_6Co_{2.18(1)}In_{0.82(1)}$ and $Sc_{10}Ni_9In_{19.44(1)}$. U_{eq} is defined as one third of the trace of the orthogonalized U_{ij} tensor.

Atom	Wyck.	Occ.	x	y	z	U_{eq}
$ScCu_4In$						
Sc	4*a*	1.00	0	0	0	48(2)
Cu	16*e*	1.00	0.62514(3)	*x*	*x*	61(2)
In	4*c*	1.00	1/4	1/4	1/4	52(2)
$Sc_6Co_{2.18(1)}In_{0.82(1)}$						
Sc1	8*n*	1.00	0.28155(13)	0.18896(13)	0	112(2)
Sc2	8*m*	1.00	0.29565(12)	0	0.31347(11)	90(2)
Sc3	8*l*	1.00	0	0.21044(13)	0.23331(13)	124(3)
Co1	4*j*	1.00	1/2	0	0.11860(12)	101(3)
Co2	4*g*	1.00	1/2	0.13087(13)	1/2	108(3)
In1	2*a*	0.64(1)	0	0	0	109(4)
Co3	2*a*	0.36	0	0	0	109
In2	2*c*	1.00	0	0	1/2	77(2)
$Sc_{10}Ni_9In_{19.44(1)}$						
Sc1	2*c*	1.00	1/4	1/4	0.6418(4)	96(8)
Sc2	2*c*	1.00	1/4	1/4	0.1606(4)	85(7)
Sc3	8*i*	1.00	1/4	0.52645(16)	0.2322(2)	87(4)
Sc4	8*j*	1.00	0.45511(12)	*x*	0.7340(2)	128(4)
Ni1	2*a*	1.00	1/4	3/4	0	85(5)
Ni2	8*i*	1.00	1/4	0.02957(11)	0.59919(15)	109(3)
Ni3	8*j*	1.00	0.59363(8)	*x*	0.89368(14)	95(3)
In1	8*g*	1.00	0.10004(4)	$-x$	0	126(2)
In2	8*h*	1.00	0.61884(5)	$-x$	1/2	195(2)
In3	8*i*	1.00	1/4	0.08039(6)	0.90360(8)	89(2)
In4a	8*i*	0.537(1)	1/4	0.86842(17)	0.76114(18)	98(4)
In4b	8*i*	0.323(3)	1/4	0.8381(3)	0.7449(3)	98(6)
In5	8*j*	1.00	0.38016(4)	*x*	0.40899(8)	87(2)

The isotypy of these scandium indides with the $MgCu_4Sn$ [15, 16], Ho_6Co_2Ga [17], and $Ho_{10}Ni_9In_{20}$ [18] type structures was already evident from the X-ray powder data. The atomic positions of the latter compounds were then taken as starting values and the structures were refined using SHELXL-97 (full-matrix least-squares on F_o^2) [19] with anisotropic atomic displacement parameters for all sites. For $ScCu_4In$ refinement of the Flack parameter [20, 21] ensured refinement of the correct absolute structure. As a check for the correct site assignment and possible defects or mixed occupancies, the occupancy parameters were refined in separate series of least-squares cycles. For $ScCu_4In$ all sites were fully occupied within two standard uncertainties. The 2*a* In1 site of Sc_6Co_2In showed a much higher isotropic displacement parameter as compared to In2, indicating a smaller scattering power at this site. Similar to $Ho_6Co_{2+x}In_{1-x}$ [22] also the 2*a* site in the scandium compound was refined with a mixed In1/Co3 occupancy, leading to the composition $Sc_6Co_{2.18}In_{0.82}$ for the investigated crystal.

The $Sc_{10}Ni_9In_{20}$ data set revealed smaller indium occupancy of only 86% for the 8*i* In4 site. Furthermore, the U_{22} parameter was five times larger than the U_{11} and U_{33} parameters, and also some residual peaks around the In4 position remained. This anomaly was associated with a very short In4–In4 distance of only 279 pm. Subsequently a split position was introduced, where both the *y* and *z* parameters were left free and also the occupancy parameter of the split site was refined independently. Only the isotropic displacement parameter of both split sites was constrained at the same value. We have then obtained a stable refinement without significant residual peaks (see Table 1) in the final difference Fourier synthesis. The sum of the freely refined occupancy parameters of both split sites was similar to the occupancy obtained from the anisotropic refinement and we obtained the composition $Sc_{10}Ni_9In_{19.44}$ for the investigated crystal. The crystal chemical consequences of the split model are discussed below. The positional parameters and interatomic distances of the three refinements are listed in Tables 2 – 4. Further details on the structure refinements are available.*

EDX analyses

The bulk samples and the single crystals measured on the diffractometer have been analyzed by EDX using a LEICA 420 I scanning electron microscope with scandium, cobalt, nickel, copper, and indium arsenide as standards. The single crystals mounted on the quartz fibre were coated with a thin carbon film. Pieces of the bulk samples were polished with different silica and diamond pastes and left unetched for the analyses in the scanning electron microscope in backscat-

*Details may be obtained from: Fachinformationszentrum Karlsruhe, D-76344 Eggenstein-Leopoldshafen (Germany), by quoting the Registry No's. CSD–416529 ($Sc_6Co_{2.18}In_{0.82}$), CSD–416530 ($Sc_{10}Ni_9In_{19.44}$), and CSD–416528 ($ScCu_4In$).

Table 3. Interatomic distances (pm) of $ScCu_4In$ and $Sc_6Co_{2.18(1)}In_{0.82(1)}$ calculated with the powder lattice parameters. Standard deviations are all equal or less than 0.2 pm. All distances within the first coordination spheres are listed. *M* denotes 64% In1 and 36% Co3 for $Sc_6Co_{2.18}In_{0.82}$.

$ScCu_4In$							
Sc:	12	Cu	291.9	Cu:	3	Cu	248.6
	4	In	304.9		3	Cu	249.2
In:	12	Cu	291.9		3	Sc	291.9
	4	Sc	304.9		3	In	291.9
$Sc_6Co_{2.18(1)}In_{0.82(1)}$							
Sc1:	2	Co1	278.0	Sc3:	1	Co2	258.3
	1	Co2	295.5		1	*M*	285.4
	1	*M*	299.8		1	Co1	289.3
	2	Sc3	327.3		1	In2	309.7
	2	Sc2	330.9		2	Sc2	315.2
	2	Sc3	331.6		2	Sc1	327.3
	1	Sc1	331.8		2	Sc2	329.3
	1	In2	334.8		2	Sc1	331.6
	2	Sc2	336.2		1	Sc3	369.5
	1	Sc1	387.4	Co1:	1	Co1	221.1
Sc2:	1	Co1	256.6		2	Sc2	256.6
	2	Co2	276.2		4	Sc1	278.0
	1	In2	314.6		2	Sc3	289.3
	2	Sc3	315.2	Co2:	1	Co2	229.8
	2	Sc3	329.3		2	Sc3	258.3
	2	Sc1	330.9		4	Sc2	276.2
	2	Sc1	336.2		2	Sc1	295.5
	1	Sc2	347.7		1	*M*	324.1
	1	Sc2	362.4	*M*:	4	Sc3	285.4
					4	Sc1	299.8
					2	Co2	324.1
				In2:	4	Sc3	309.7
					4	Sc2	314.6
					4	Sc1	334.8

tering mode. No impurities were detected *via* EDX. The analyses, 29 ± 2 at.-% Sc : 23 ± 2 at.-% Ni : 48 ± 2 at.-% In for $Sc_{10}Ni_9In_{19.44}$, 18 ± 2 at.-% Sc : 63 ± 2 at.-% Cu : 19 ± 2 at.-% In for $ScCu_4In$, and 69 ± 2 at.-% Sc : 20 ± 2 at.-% Co : 11 ± 2 at.-% In for $Sc_6Co_{2.18}In_{0.82}$ were, within the experimental uncertainties, close to the compositions derived from the structure refinements.

Discussion

Three new scandium-transition metal-indides, *i.e.* Sc_6Co_2In, $Sc_{10}Ni_9In_{20}$ and $ScCu_4In$ were synthesized and their crystal structures were refined on the basis of single crystal diffractometer data. Among these compounds, $ScCu_4In$ adopts the simplest structure. The copper compound crystallizes with the cubic $MgCu_4Sn$ type structure [15, 16], a ternary ordered variant of the cubic Laves phase $MgCu_2$. This structure type was also observed for isotypic $ScNi_4In$ [3].

Table 4. Interatomic distances (pm), calculated with the single crystal lattice parameters of $Sc_{10}Ni_9In_{19.44(1)}$. The too short In–In distances that are affected by the In4 split positions are put in brackets. Standard deviations are all equal or less than 0.3 pm.

Sc1:	4	Ni2	286.3	In2:	2	Ni2	269.7
	4	In5	314.0		2	In4b	280.3
	4	In3	318.3		2	In4a	286.6
Sc2:	4	Ni3	288.7		2	Sc4	310.4
	4	In3	315.2		2	Sc3	314.3
	4	In5	323.2		2	In5	317.7
Sc3:	4	Ni3	277.2		2	In2	337.7
	2	In5	296.7	In3:	2	Ni3	270.2
	2	In1	297.4		1	Ni2	277.1
	2	In4b	310.0		1	In4a	300.6
	2	In2	314.3		2	Sc4	307.1
	1	In3	321.6		2	In3	308.8
	2	In4a	325.8		2	In1	313.9
Sc4:	1	Ni3	289.1		1	Sc2	315.2
	2	Ni2	290.4		1	Sc1	318.3
	2	In3	307.1		1	Sc3	321.6
	2	In1	308.6		1	In4b	342.0
	2	In2	310.4	In4a:	1	In4b	[39.4]
	1	In5	318.3		1	Ni2	252.1
	1	In5	325.5		1	Ni1	260.6
Ni1:	4	In4b	252.6		1	In4b	[266.3]
	4	In4a	260.6		2	In2	286.6
	4	In1	273.0		2	In1	289.1
Ni2:	1	In4a	252.1		1	In3	300.6
	2	In5	264.4		1	In4a	304.9
	2	In2	269.7		2	Sc3	325.8
	1	In3	277.1		2	Sc4	349.2
	1	In4b	278.2	In4b:	2	In4a	[39.4]
	1	Sc1	286.3		1	In4b	[226.9]
	2	Sc4	290.5		1	Ni1	252.6
Ni3:	2	In1	266.6		1	In4a	266.3
	2	In3	270.2		1	Ni2	278.2
	1	In5	272.0		2	In2	280.2
	2	Sc3	277.2		2	In1	307.5
	1	Sc2	288.7		2	Sc3	310.0
	1	Sc4	289.1		1	In3	342.0
In1:	2	Ni3	266.6	In5:	2	Ni2	264.4
	1	Ni1	273.0		1	Ni3	272.0
	2	In4a	289.1		2	Sc3	296.7
	2	Sc3	297.4		1	Sc1	314.0
	2	In4b	307.5		2	In2	317.7
	2	Sc4	308.6		1	Sc4	318.3
	2	In3	313.9		1	Sc2	323.2
					1	Sc4	325.5
					2	In5	335.2

As emphasized in Fig. 1, the copper atoms in $ScCu_4In$ build up a three-dimensional network of corner-sharing $Cu_{4/4}$ tetrahedra. The scandium and indium atoms show an ordering on the magnesium site of the Laves phase, resulting in a translationengleiche symmetry reduction of index 2 from space group $Fd\bar{3}m$ to $F\bar{4}3m$. Due to the symmetry reduction we observe a small distortion within the tetrahedral network, lead-

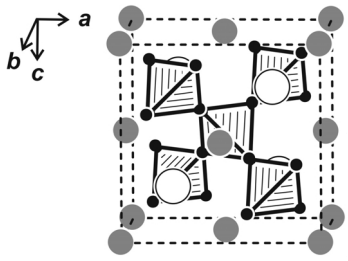

Fig. 1. The crystal structure of $ScCu_4In$. The scandium, copper, and indium atoms are drawn as medium gray, black filled, and open circles, respectively. The three-dimensional network of corner-sharing [Cu_4] tetrahedra is emphasized.

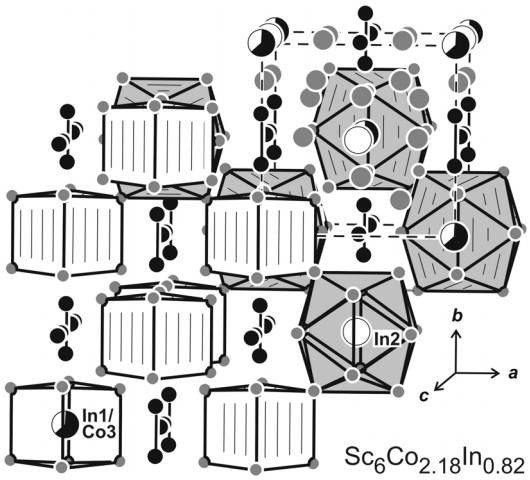

Fig. 2. View of the $Sc_6Co_{2.18}In_{0.82}$ structure approximately along the *c* axis. The scandium, cobalt, and indium atoms are drawn as medium gray, black filled, and open circles, respectively. The distorted cube-like (In1/Co3) and icosahedral (In2) coordination polyhedra and the two crystallographically independent Co_2 dumb-bells are emphasized. For details see text.

ing to slightly different Cu–Cu distances of 248.6 and 249.2 pm, close to the Cu–Cu distance in *fcc* copper (256 pm) [23]. The tetrahedral copper substructure leaves large voids of coordination number 16 for the scandium $(12\,\mathrm{Cu} + 4\,\mathrm{In})$ and indium $(12\,\mathrm{Cu} + 4\,\mathrm{Sc})$ atoms. For a more detailed discussion on the crystal chemistry and chemical bonding in such Laves phases we refer to recent review articles [24 – 27, and ref. therein].

The crystal structure of $Sc_6Co_{2.18}In_{0.82}$ is presented in Fig. 2. This indide crystallizes with the orthorhombic Ho_6Co_2Ga type structure, space group *Immm*. So far, this structure type has been observed for the series of gallides RE_6Co_2Ga and RE_6Ni_2Ga [28], some stannides RE_6Ni_2Sn [28] and the indides $RE_6Co_{2+x}In_{1-x}$

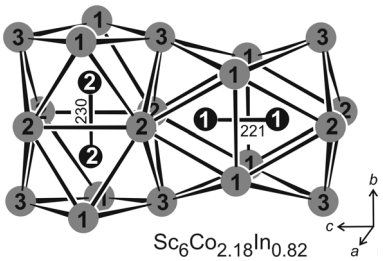

Fig. 3. Cutout of the $Sc_6Co_{2.18}In_{0.82}$ structure. The condensation of the distorted trigonal prisms around the cobalt atoms is emphasized.

(*RE* = Y, Sm, Gd–Tm, Lu) [22, 29, 30]. Similar to the holmium compound [23], also for the scandium compound we observed a small range of homogeneity $Sc_6Co_{1+x}In_{1-x}$.

The complex structure is best described by the orthorhombic body-centered packing of two different motifs, *i. e.* distorted $In2Sc_{12}$ icosahedra and distorted $In1Sc_8$ cubes. Each of these packings leaves voids that are filled by Co_2 dumb-bells: Co1–Co1 at 221 pm extending along *c* and Co2–Co2 at 230 pm extending along *b*. Both Co–Co distances are significantly smaller than the average Co–Co distance of 250 pm in *hcp* cobalt [23], and we can assume strong Co–Co bonding within these units.

Fig. 3 shows a cutout for the trigonal prismatic coordination of the cobalt atoms by scandium. Since the cobalt atoms form pairs, we consequently observe two distorted AlB_2 related slabs in the $Sc_6Co_{2.18}In_{0.82}$ structure. These trigonal prisms are capped on the rectangular sides by two scandium atoms and one cobalt atom, leading to coordination number 9, typically observed for the transition metal atoms in such indide structures [2].

As expected from the high scandium content, we observe a variety of Sc–Sc contacts with Sc–Sc distances ranging from 315 to 387 pm. Each of the three crystallographically independent scandium atoms has at least two scandium neighbours at Sc–Sc distances shorter than the average Sc–Sc distance of 328 pm in *hcp* scandium [23]. In view of the high scandium content, the segregation of the cobalt atoms into Co2 dumb-bells is remarkable. A similar situation was observed for the $RE_5Ni_6In_{11}$ indides [31–33].

The most complex structure among these three scandium indides is $Sc_{10}Ni_9In_{19.44}$. This compound crystallizes with the tetragonal $Ho_{10}Ni_9In_{20}$ type, also observed for *RE* = Tb, Dy, Er, Tm, Lu [18, 34]

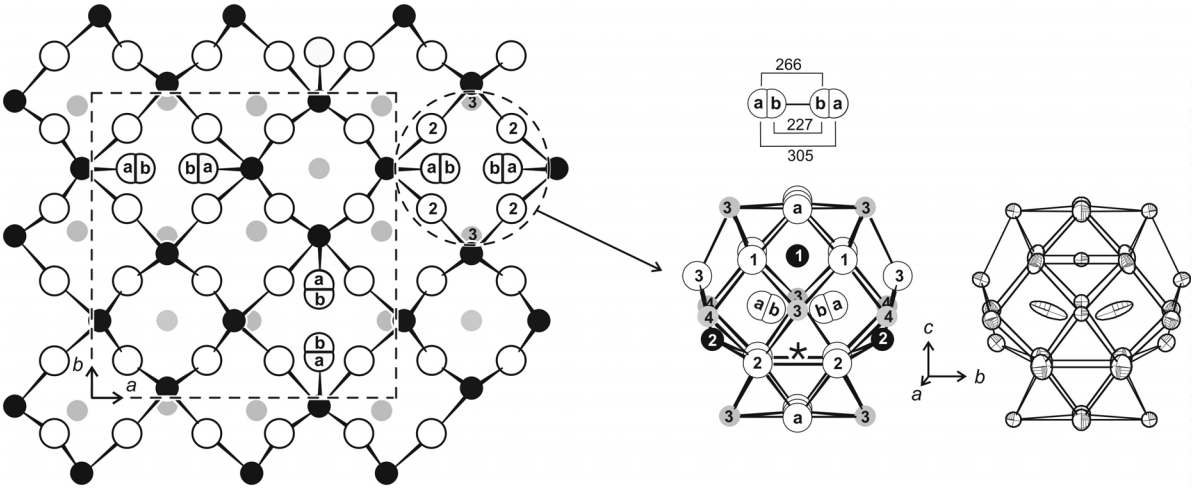

Fig. 4. Projection of the $Sc_{10}Ni_9In_{19.44}$ structure onto the *xy* plane (left-hand drawing; for clarity, only half the structure along *c* is shown). The scandium, nickel, and indium atoms are drawn as medium gray, black filled, and open circles, respectively. The split In4 site is designated with *a* and *b*. The local coordination of these sites is presented in the middle (split model) and right-hand (ellipsoidal presentation) drawing. The In4a/b–In4a/b distances resulting from the split refinement are also given. The asterisk marked in the middle drawing indicates a position that can be occupied in some $Ho_{10}Ni_{9\pm x}In_{20}$ type compounds. For details see text.

and the series of rhodium compounds $RE_{10}Rh_9In_{20}$ (*RE* = Y, Tb–Tm, Lu) [35]. However, $Tb_{10}Ni_{9.34}In_{20}$ and $Dy_{10}Ni_{9.32}In_{20}$ and the $RE_{10}Rh_{9\pm x}In_{20}$ indides show a significant difference when compared with $Sc_{10}Ni_9In_{19.44}$ described herein. With the larger rare earth metals one observes one additional nickel or rhodium site within a trigonal prism. This position, marked with an asterisk in Fig. 4, is not occupied in $Sc_{10}Ni_9In_{19.44}$. This is a direct consequence of the small size of the scandium atoms. An occupancy of that position would result in very short Ni–In distances of 240 pm. The crystal chemistry of this structure type was described in detail already for the $RE_{10}Rh_{9\pm x}In_{20}$ series [35]. Therefore, herein we focus only on the peculiarities of the $Sc_{10}Ni_9In_{19.44}$ structure.

Besides the non-occupied trigonal prism, the small size of the scandium atoms also has a drastic effect on the In4 position. Refinement of the occupancy parameter revealed an occupancy of only 86%, and a small range of homogeneity $Sc_{10}Ni_9In_{20-x}$ is likely to exist. Furthermore, the In4 atoms show an extremely anisotropic displacement (right-hand part of Fig. 4). A reasonable refinement of this structure without significant residual peaks in the difference Fourier synthesis was only possible with an In4 split position with free *y* and *z* parameters. The split positions In4a and In4b show shorter and longer In4*a*/*b*–In4*a*/*b* distances. The In4*b* sites cannot simultaneously be occupied, since too short distances of 227 pm would result. The refined occupancy parameters of In4a (54%) and In4*b* (32%) are consistent with these findings. The In4b site shows the smaller occupancy.

The In4a–In4b (266 pm) and In4*a*–In4*a* (305 pm) distances are also shorter than the In–In distances in tetragonal body-centered indium (4×325 and 8×338 pm) [23]. Such shorter In–In distances have repeatedly been observed in ternary indides. Recent examples are the structures of $La_4Pd_{10}In_{21}$ [36] (286 and 289 pm), $EuRh_2In_8$ [37] (288 and 290 pm) or La_3In_4Ge [38] (287 pm).

Acknowledgements

We thank H.-J. Göcke for the work at the scanning electron microscope. This work was supported by the Deutsche Forschungsgemeinschaft.

[1] J. Emsley, The Elements, Oxford University Press, Oxford (1999).

[2] Ya. M. Kalychak, V. I. Zaremba, R. Pöttgen, M. Lukachuk, R.-D. Hoffmann, Rare Earth-Transition Metal-Indides, in K. A. Gschneidner (Jr.), V. K. Pecharsky, J.-C. Bünzli, Handbook on the Physics and Chemistry of Rare Earths, Vol. 34, Chapter 218, p. 1 – 133, Elsevier, Amsterdam (2005).

[3] V. I. Zaremba, V. M. Baranyak, Ya. M. Kalychak, Vestn. Lvov Univ., Ser. Khim. **25**, 18 (1984).
[4] N. N. Kiseleva, Izv. Akad. Nauk. SSSR, Metally **2**, 213 (1987).
[5] A. E. Dwight, C. W. Kimball, J. Less-Common Met. **127**, 179 (1987).
[6] B. T. Matthias, E. Corenzwit, J. M. Vandenberg, H. Barz, M. B. Maple, R. N. Shelton, J. Less-Common Met. **46**, 339 (1976).
[7] R. Pöttgen, R. Dronskowski, Z. Anorg. Allg. Chem. **622**, 355 (1996).
[8] F. Hulliger, J. Alloys Compd. **232**, 160 (1996).
[9] Ya. V. Galadzhun, V. I. Zaremba, H. Piotrowski, P. Mayer, R.-D. Hoffmann, R. Pöttgen, Z. Naturforsch. **55b**, 1025 (2000).
[10] M. Lukachuk, B. Heying, U. Ch. Rodewald, R. Pöttgen, Heteroatom Chem. **16**, 364 (2005).
[11] M. Lukachuk, V. I. Zaremba, R.-D. Hoffmann, R. Pöttgen, Z. Naturforsch. **59b**, 182 (2004).
[12] V. P. Urvachev, V. P. Polyakova, E. M. Savitskii, in E. M. Savitskii (ed.): Splavy Redkikh Metallov s Osobymi Fizicheskimi Svojstvami, p. 141, Redkozemelnye I Blagorodnye Metally, Nauka, Moscow (1983).
[13] R. Pöttgen, Th. Gulden, A. Simon, GIT Labor Fachzeitschrift **43**, 133 (1999).
[14] K. Yvon, W. Jeitschko, E. Parthé, J. Appl. Crystallogr. **10**, 73 (1977).
[15] E. I. Gladyshevskii, P. I. Krypiakevych, M. Yu. Teslyuk, Dokl. AN SSSR **85**, 81 (1952).
[16] K. Osamura, Y. Murakami, J. Less-Common Met. **60**, 311 (1978).
[17] R. E. Gladyshevsky, Yu. N. Grin, Ya. P. Yarmolyuk, Dopov. Akad. Nauk. Ukr. RSR, Ser. A **45**, 67 (1983).
[18] V. I. Zaremba, V. K. Bels'kii, Ya. M. Kalychak, V. K. Pecharsky, E. I. Gladyshevskii, Dopov. Akad. Nauk Ukr. RSR, Ser. B 42 (1987).
[19] G. M. Sheldrick, SHELXL-97, Program for Crystal Structure Refinement, University of Göttingen, Germany (1997).
[20] H. D. Flack, G. Bernadinelli, Acta Crystallogr. **55A**, 908 (1999).
[21] H. D. Flack, G. Bernadinelli, J. Appl. Crystallogr. **33**, 1143 (2000).
[22] Ya. M. Kalychak, V. I. Zaremba, P. Yu. Zavalij, Z. Kristallogr. **208**, 380 (1993).
[23] J. Donohue, The Structures of the Elements, Wiley, New York (1974).
[24] A. Simon, Angew. Chem. **95**, 94 (1983).
[25] R. Nesper, Angew. Chem. **103**, 805 (1991).
[26] R. L. Johnston, R. Hoffmann, Z. Anorg. Allg. Chem. **616**, 105 (1992).
[27] R. Nesper, G. J. Miller, J. Alloys Compd. **197**, 109 (1993).
[28] O. M. Sichevich, L. P. Komarovskaja, Yu. N. Grin, Ya. P. Yarmolyuk, R. V. Skolozdra, Ukr. Fiz. Zh. **29**, 1342 (1984).
[29] Ya. M. Kalychak, unpublished results.
[30] F. Canepa, M. Napoletano, P. Manfrinetti, F. Merlo, J. Alloys Compd. **334**, 34 (2002).
[31] Ya. M. Kalychak, P. Yu. Zavalii, V. M. Baranyak, O. V. Dmytrakh, O. I. Bodak, Kristallografiya **32**, 1021 (1987).
[32] J. Tang, K. A. Gschneidner (Jr.), S. J. White, M. R. Roser, T. J. Goodwin, L. R. Corruccini, Phys. Rev. B **52**, 7328 (1995).
[33] R. Pöttgen, R.-D. Hoffmann, R. K. Kremer, W. Schnelle, J. Solid State Chem. **142**, 180 (1999).
[34] V. I. Zaremba, I. R. Muts, U. Ch. Rodewald, V. Hlukhyy, R. Pöttgen, Z. Anorg. Allg. Chem. **630**, 1903 (2004).
[35] M. Lukachuk, U. Ch. Rodewald, V. I. Zaremba, R.-D. Hoffmann, R. Pöttgen, Z. Anorg. Allg. Chem. **630**, 2253 (2004).
[36] V. I. Zaremba, U. Ch. Rodewald, Ya. M. Kalychak, Ya. V. Galadzhun, D. Kaczorowski, R.-D. Hoffmann, R. Pöttgen, Z. Anorg. Allg. Chem. **629**, 434 (2003).
[37] R. Pöttgen, D. Kußmann, Z. Anorg. Allg. Chem. **627**, 55 (2001).
[38] A. M. Guloy, J. D. Corbett, Inorg. Chem. **35**, 2616 (1996).